International Journal of Cardiology 285 (2019) 80–85

Contents lists available at ScienceDirect

International Journal of Cardiology

journal homepage: www.elsevier.com/locate/ijcard

Diagnosis of pulmonary hypertension using spectral-detector CT

Jan Robert Kröger [a,*], Felix Gerhardt [b], Daniel Dumitrescu [b], Stephan Rosenkranz [b], Matthias Schmidt [c], David Maintz [a], Alexander C. Bunck [a]

[a] University of Cologne, Faculty of Medicine and University Hospital Cologne, Department of Radiology, Germany
[b] University of Cologne, Faculty of Medicine and University Hospital Cologne, Department of Cardiology, Germany
[c] University of Cologne, Faculty of Medicine and University Hospital Cologne, Department of Nuclear-Medicine, Germany

ARTICLE INFO

Article history:
Received 2 October 2018
Received in revised form 4 February 2019
Accepted 11 March 2019
Available online 13 March 2019

Keywords:
Pulmonary hypertension
Pulmonary embolism
CT angiography
Spectral-detector CT
Dual-energy CT

ABSTRACT

Objectives: To evaluate the value of spectral-detector CT (SDCT) in the diagnosis of chronic thromboembolic pulmonary hypertension (CTEPH), its differentiation against other etiologies of pulmonary hypertension (PH) and in the prediction of disease severity.
Materials and methods: 60 patients with suspected PH underwent SDCT. Additional diagnostic tests in accordance with the ESC guidelines including right heart catherization and VQ-SPECT were performed. After full diagnostic work-up patients were classified as: 21 precapillary PH, 5 postcapillary PH, 6 combined pre- and postcapillary PH, 19 CTEPH, 9 no PH. SDCT examinations were analyzed by two blinded readers deciding on the diagnosis of CTEPH and scoring the extent of perfusion abnormalities on iodine density images. An additional reading was performed using conventional CTPA images only.
Results: With access to SDCT data, both readers reached a sensitivity of 100% for the diagnosis of CTEPH with a specificity of 95.1% and 87.8%. On analysis of conventional CTPA images alone, specificity and diagnostic confidence decreased for both readers (Specificity 90.2 and 85.3%) while sensitivity dropped for the less experienced reader only (Sensitivity 78.9%). Patients with PH showed significantly more perfusion abnormalities than patients without PH (16.6 ± 8.4 vs. 9.5 ± 8.9 $p < 0.001$) and the extent of perfusion abnormalities correlated with the mean pulmonary artery pressure ($r = 0.37$ $p = 0.008$).
Conclusions: SDCT offers confident identification of patients with CTEPH and enables a comprehensive analysis of pulmonary vasculature, pulmonary perfusion and the lung parenchyma in a single examination for patients with suspected PH.

1. Introduction

Pulmonary hypertension (PH) is characterized by elevated pressure in the pulmonary artery. Diagnosis and assessment of disease severity is based on right heart catheterization (RHC) with pressure measurements in the pulmonary artery and the right heart, most importantly the main pulmonary artery pressure (mPAP) [1]. By additional hemodynamic parameters RHC differentiates between pre-capillary PH, post-capillary PH or combined pre-capillary and post-capillary PH [1] but additional information is needed to categorize PH further based on its pathogenesis according to the Nice Classification [2]. Chronic thromboembolic pulmonary hypertension (CTEPH) is often overlooked [3], but the accurate identification of this entity is crucial because these patients can potentially be cured by surgical thrombendarteriectomy [4] or benefit from balloon pulmonary angioplasty [5,6]. To screen for CTEPH, current guidelines recommend ventilation/perfusion (V/Q)-scintigraphy [1] because of its excellent sensitivity for detection of mismatched perfusion defects suggestive of CTEPH [7]. If V/Q-scintigraphy reveals signs of probable CTEPH, CT pulmonary angiography (CTPA) is performed to confirm abnormalities like partial or complete vessel occlusion and stenoses of the pulmonary artery [1,8].

Recent studies have shown that CTPA with modern CT scanners can yield sensitivities and specificities similar to V/Q-scintigraphy for the diagnosis of CTEPH [9,10]. The application of dual-energy CT (DECT) is particularly appealing because iodine density images (IDIs) provide information on pulmonary perfusion similar to perfusion scintigraphy [11–14]. Moreover, DECT has the potential to differentiate subtypes of PH based on perfusion characteristics [15,16] and to estimate the clinical severity of CTEPH [17]. Additionally DECT data can be used to

Abbreviations: PH, pulmonary hypertension; CTEPH, chronic thromboembolic pulmonary hypertension; CT, computed tomography; SDCT, spectral detector computed tomography; V/Q, ventilation/perfusion; RHC, right heart catheterization; mPAP, main pulmonary artery pressure; CTPA, CT pulmonary angiography; DECT, dual energy CT; IDI, iodine density image; AA, ascending aorta; MPA/RPA/LPA, main/right/left pulmonary artery; RV/LV, right/left ventricle; cpc-PH, combined pre- and postcapillary PH.

* Corresponding author at: University Hospital Cologne, Department of Radiology, Kerpener Str. 62, 50937 Cologne, Germany.
E-mail address: jan.kroeger@uk-koeln.de (J.R. Kröger).

https://doi.org/10.1016/j.ijcard.2019.03.018
0167-5273/

reconstruct monoenergetic images at lower keV values [18] which increase the iodine contrast and thus are helpful when reading CT angiographic studies.

In contrast to the tube-based technical solutions for dual-energy CT, recently the first CT scanner with detector-based solution referred to as spectral detector CT (SDCT) became available. This technique has the advantage of exact spatial and angular congruence of high and low energy projection data [19]. First results have shown very good image quality for CT examinations of the chest using SDCT [20] and in the pulmonary artery an improvement of vessel to thrombus contrast was shown for SDCT derived monoenergetic images [21].

We aimed to evaluate if the additional information provided by spectral-detector CT (SDCT) is helpful in the diagnosis of PH, the differentiation of its subgroups and in the prediction of disease severity.

2. Material and methods

2.1. Patient population

The retrospective study was approved by our institutional ethics committee and the need for informed consent for study enrollment was waived due to the retrospective nature of data analysis.

A retrospective data base search identified 60 consecutive patients that underwent CTPA for the evaluation of possible PH on a spectral detector CT (SDCT, IQon, Philips Healthcare, Best, The Netherlands) between June 2016 and December 2017. All these patients had suspected PH and were admitted to the department of cardiology at our hospital for further testing.

Patients underwent additional diagnostics tests in accordance with the 2015 ESC/ERS guidelines for the diagnosis of pulmonary hypertension [1] with all patients undergoing RHC. In 53 patients CT examination and RHC were performed within 5 days (interval between the two examinations: 1.2 ± 1.1 days, Median 1 day, Range 0–5 days) and results were analyzed for correlation. In seven patients, however, the latest RHC was >10 days apart from the CT examination and thus their results were excluded from correlation analysis between RHC derived values and SDCT scores.

55 patients underwent additional V/Q-SPECT at our clinic. In 5 patients V/Q-scintigraphy was done at an external institution and data sets were not available for analysis. None of the patients without available V/Q-SPECT was diagnosed with CTEPH. 14 patients received invasive pulmonary angiography. Patients were classified and final diagnosis was set by expert consensus based on all diagnostic tests.

2.2. Image acquisition and reconstruction

CT data were acquired on a 128-row spectral detector CT. According to our institutional standard for CTPA studies, all patients received 50 ml of contrast media (300 mg Iodine/ml, Accupaque, GE Healthcare, Chicago, Illinois, USA) followed by a 40 ml NaCl flush were injected intravenously with a flow rate of 4 ml/s. Scanning was initiated with a delay of 4.9 s after an attenuation of 150 HU was reached in the MPA. Scanning and reconstruction parameters were: slice collimation 0.625 mm; rotation time 0.33 s; tube potential 120 kV, automatic tube current modulation was used; reconstructed axial slice thickness 1 mm; reconstructed axial slice overlap 0.5 mm; pixel matric 512 × 512.

2.3. Image analysis

Datasets were analyzed using the CT Spectral Viewer integrated in the Intellispace Portal environment (ISP Version 10, Philips Healthcare, Best, The Netherlands) which allowed for simultaneous viewing of conventional, monoenergetic and iodine density images. Two radiologists with 4 and 11 years' experience in reading CTPA studies and blinded for any clinical information or additional imaging studies evaluated the datasets. While overall experience of the two radiologist regarding CTPA was different both had similar experience in reading SDCT images. Both readers rated image quality on a 5-step Likert-scale (1: not diagnostic, 2: poor, 3: moderate, 4: good 5: perfect image quality). Furthermore, both readers stated whether they suspected a patient of suffering from CTEPH (yes or no) and rated their diagnostic confidence on a 5-step Likert-scale (1: very uncertain, 2: uncertain, 3: intermediate, 4: confident, 5: definite diagnosis). Diagnostic criteria for CTEPH were partial or complete occlusion of pulmonary vessels by chronic emboli and/or vessel obliteration on CTPA images and/or typical segmental or regional perfusion defects on IDIs [8,22]. Both readers determined the extent of pathologic changes in iodine distribution on IDIs for each pulmonary segment and stated whether less or >50% of each segment were affected (corresponding to a score of 0 if no perfusion defect was present, 1 point: <50% of the segment with perfusion defect, or 2 points: >50% of the segment with perfusion defect). Abnormalities in iodine distribution were rated as patchy, wedge-shaped embolic defects or large regional defects (see Fig. 1). The scores for perfusion deficits that could be attributed to the presence of pulmonary emphysema, based on an assessment of lung window images and IDIs, were excluded from further quantitative analysis (see Fig. 1), however the patients were included in all further analysis. Scores for every segment were summed up to give an overall severity score of perfusion abnormalities per patient. Furthermore, scores by both readers were averaged for each patient.

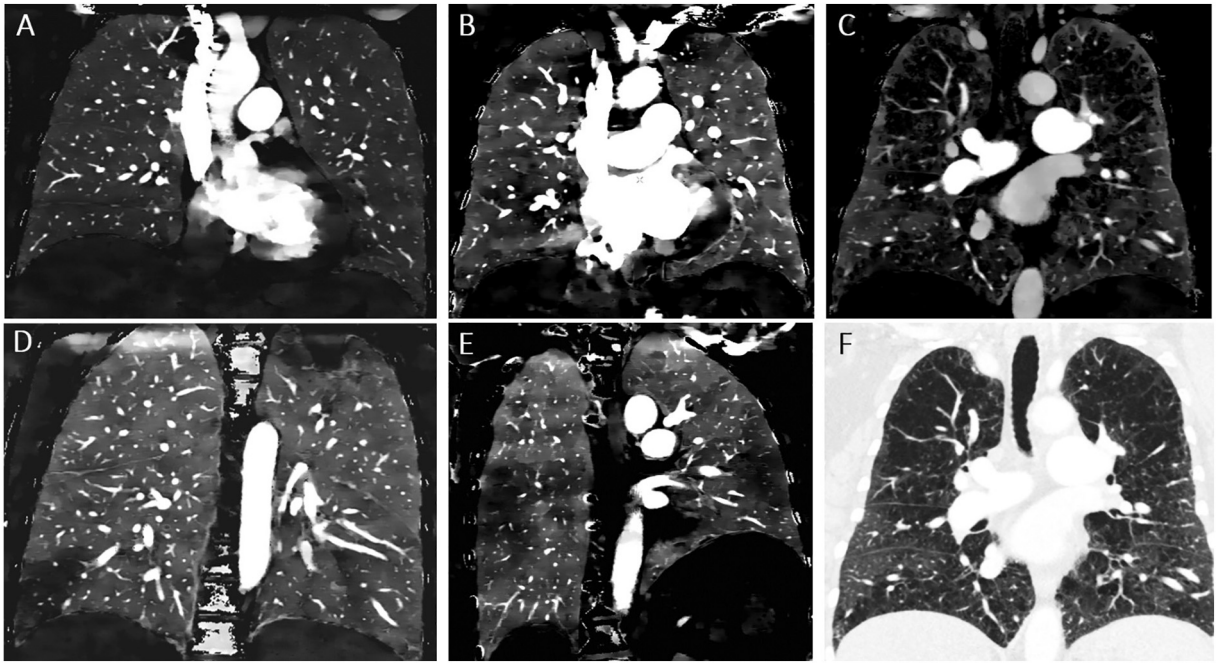

Fig. 1. Different types of pulmonary perfusion on iodine density images. Different types of pulmonary perfusion found in our cohort shown on iodine density images. A depicts a homogenous distribution of iodine regarded as normal. B shows patchy type abnormalities meaning there are interspersed areas of reduced perfusion which do not correspond to a clear vascular territory in between areas of normal perfusion. C shows perfusion defects caused by destruction of lung parenchyma in a patient with pulmonary emphysema. These changes can be clearly attributed to pulmonary emphysema when comparing iodine density images and lung window images as depicted in F. D shows wedge-shaped embolic defects which can attributed to the occlusion of a subsegmental vessel. More extensive areas of hypoperfusion that extend to a pulmonary segment or more as seen in E were termed regional defects.

6 weeks after the first reading, both readers reread all conventional CTPA images, this time without additional access to monoenergetic or iodine density images. Again, both readers stated whether findings on the CTPA images were consistent with a diagnosis of CTEPH and rated their diagnostic confidence.

Finally, an additional consensus reading was performed for those cases in which only one reader suspected a patient of suffering from CTEPH.

Additionally, one reader measured the diameters of the ascending aorta (AA), the main pulmonary artery (MPA), the right and left pulmonary artery (RPA/LPA) as well as the diameter of the right and left ventricle (RV and LV) on a four-chamber view. Attenuation in the AA and MPA was measured.

2.4. Statistical analysis

Statistical analysis was performed using SPSS Statistics 25 (IBM, Armonk NY, USA). Shapiro-Wilk test suggested to discard normal distribution. Differences between groups were tested for significance using the Mann-Whitney-*U* test. Differences in scoring between the two readers as well as diagnostic confidence between the first and second reading was compared using Wilcoxon signed-rank test. Correlation was calculated using the Spearman-Rho coefficient. Interobserver agreement was estimated by the Cohen-Kappa. A p-value of <0.05 was considered statistically significant.

3. Results

3.1. Patient population

60 consecutive patients with a mean age of 64.6 ± 15.1 years were included.

By expert consensus based on all diagnostic tests, patients were classified based on all diagnostics tests as: 21 precapillary PH, 5 postcapillary PH, 6 combined pre- and postcapillary PH, 19 CTEPH. In 9 patients who underwent CTPA because of suspected PH, PH was eventually excluded. For this paper we differentiated patients with CTEPH from patients with precapillary PH of other etiologies.

3.2. Image quality

Both readers rated overall image quality as good or very good on the 5-point Likert-scale (Reader 1: 4.7 ± 0.7; Reader 2: 3.7 ± 0.6) and only in 1, respectively, in 2 patients image quality was rated as poor (score of 2).

Attenuation in the MPA was 349.8 ± 128.7 HU ranging from 134 to 1051 HU. In contrast, attenuation in the ascending aorta was 214.7 ± 57.9 HU thus showing predominantly contrast enhancement of the pulmonary vasculature with a significant amount of systemic arterial enhancement.

3.3. Diameter assessment

Patients with PH had significantly greater diameters of the MPA and RPA compared to patients without PH (MPA: 3.4 ± 0.5 cm vs. 2.8 ± 0.3 cm, $p < 0.001$; RPA: 2.7 ± 0.5 cm vs. 2.3 ± 0.3 cm, $p = 0.003$). PH patients without CTEPH showed a weak but significant correlation between the diameter of the MPA and the mPAP ($r = 0.41$; $p = 0.036$). In patients with CTEPH these two parameters were not significantly correlated ($r = 0.38$; $p = 0{,}164$). Additional anatomic measurements are available as electronic Supplementary material 1.

3.4. Diagnosis of CTEPH

For the reading with access to all image types reader agreement for a diagnosis of CTEPH was excellent with a Cohen-Kappa of 0.89. Sensitivity for the detection of CTEPH was 100% for both readers with a specificity of 95.1% and 87.8% respectively. In comparison, sensitivity and specificity for V/Q-SPECT were similar with 100% and 92.7%.

2 patients without CTEPH were classified as possible CTEPH by both readers. One of these patients had a pulmonary embolism which was also seen in V/Q-SPECT but did not have significantly elevated pulmonary artery pressure and thus was not diagnosed as PH. The other patient had a pulmonary embolism, but hemodynamics indicated a postcapillary PH and thus he was not classified as CTEPH. Reader 2 identified vascular abnormalities in 3 more patients which were not identified by Reader 1 or V/Q-SPECT. In an additional consensus reading these patients showed focal dystelectasis or scarring and bronchiectasis with reduced contrast of the associated vessel which were viewed as likely not thromboembolic.

In V/Q- Scintigraphy two patients were suspected to have pulmonary emboli who, based on the CT images, were rated by both readers as not likely to have a diagnosis of CTEPH. One of the patients underwent additional pulmonary angiography which ruled out pulmonary emboli. The other patient did not show evaluated pulmonary artery pressure and PH was ruled out.

In comparison, the second reading with access to only the conventional CTPA images resulted in lower sensitivity and specificity for reader 1 with 78.9% and 90.2% while for reader 2 sensitivity remained at 100% whereas specificity decreased to 85.3%. Moreover, reader agreement was worse on the second reading with a Cohen-Kappa of 0.71.

Diagnostic certainty was rated as high by both readers for the reading with access to all image types and was significantly lower for the second reading with access to conventional CTPA images only (Reader 1: 4.7 ± 0.7 vs. 3.8 ± 1.2, $p < 0.001$; Reader 2: 4.6 ± 0.8 vs. 4.1 ± 1.0, $p < 0.001$).

3.5. Iodine density images

Patients with confirmed PH had significantly more abnormalities in iodine distribution than patients without PH (see Table 1). There was a weak but significant correlation between the extent of abnormalities in iodine distribution and the mPAP ($r = 0.37$; $p = 0.008$, see also electronic Supplementary material 2) for all PH patients. In CTEPH patients alone, however, the correlation between the extent of perfusion abnormalities and the mPAP was not significant ($r = 0.34$; $p = 0.904$).

Table 1
Comparison of perfusion abnormalities between different patient groups. Significant differences between groups are marked as: * No PH vs. All PH, + No PH vs. CTEPH, # PH but no CTEPH vs. CTEPH, § precapillary PH vs. cpc-PH, $ precapillary PH vs. CTEPH, ^ postcapillary PH vs. CTEPH, € cpc-PH vs. CTEPH.
Level of significance is indicated by the number of symbols, e.g. * = $p < 0.05$, ** $p = 0.005$, *** = $p < 0.001$.

	No PH	All PH	PH but no CTEPH	Precapillary PH	Postcapillary PH	Cpc-PH	CTEPH
Overall perfusion abnormalities	9.5 ± 8.9*;+++	16.6 ± 8.4*	13.0 ± 7.3###	11.6 ± 7.5§;$$$	13.0 ± 7.9^^	18.1 ± 4.5$	22.7 ± 6.6+++;###;$$$;^^
Patchy perfusion abnormalities	7.7 ± 7.7	10.1 ± 6.6	11.7 ± 6.8#	10.5 ± 7.2	13.0 ± 7.9	15.1 ± 3.2€€	7.4 ± 5.4#;€€
Wedge-shaped embolic perfusion defects	0.1 ± 0.2	0.6 ± 1.4	0.4 ± 1.2#	0.3 ± 0.9	0.0 ± 0.0	1.0 ± 2.2	0.9 ± 1.6#
Regional perfusion defects	1.7 ± 5.9+++	5.9 ± 9.0	0.9 ± 2.0###	0.8 ± 1.8$$$	0.0 ± 0.0^^^	2.0 ± 3.1€€	14.3 ± 10.0+++;###;$$$;^^^;€€
Wedge-shaped embolic and regional perfusion defects combined	1.8 ± 2.6+++	6.5 ± 9.3	1.3 ± 2.6###	1.1 ± 2.5$$$	0.0 ± 0.0^^^	3.0 ± 3.3€€	15.3 ± 9.9+++,###;$$$;^^^;€€

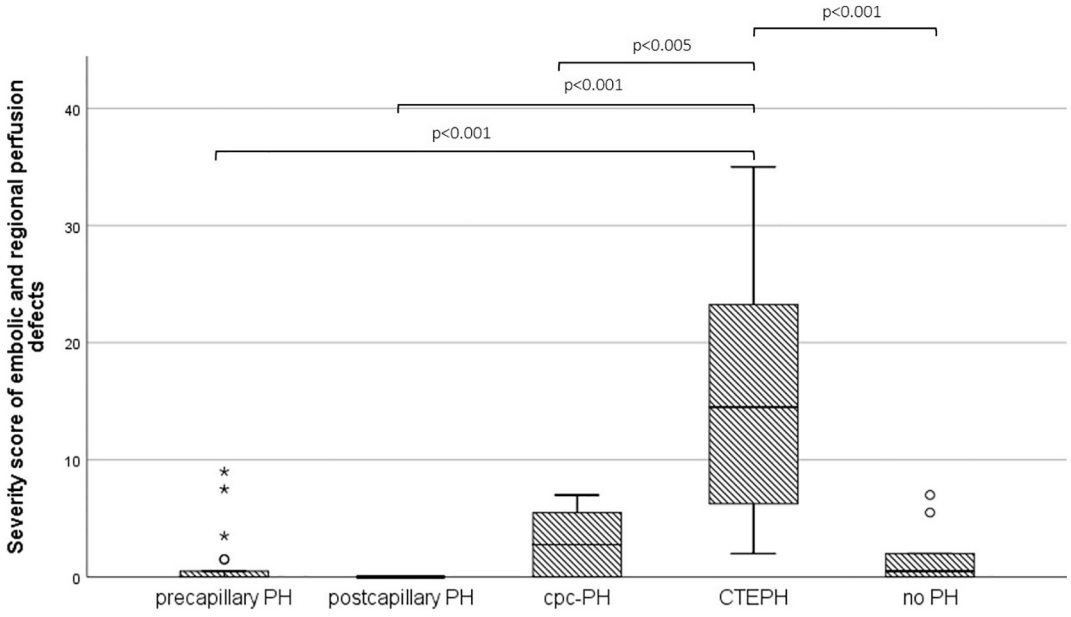

Fig. 2. Extent of embolic and regional perfusion defects between patient groups. These perfusion defects are significantly more extensive in patients with CTEPH.

On analysis of perfusion patterns, patients with CTEPH showed significantly more abnormalities in iodine distribution compared to patients with PH of any other cause (see Table 1) and significantly more wedge-shaped embolic defects and regional defects, in particular (see Table 1, electronic Supplementary material 3 and Fig. 2). This was true for the mean score averaged between the two readers as well as for each reader independently.

Conversely, patients without CTEPH had significantly more patchy abnormalities (see Table 1).

The overall score for abnormalities in iodine distribution as well as the score for embolic and regional perfusion defects were significantly different between the two readers (13.6 ± 10.3 vs. 17.5 ± 8.6; $p < 0.001$ and 4.5 ± 9 vs. 7.1 ± 9.4; $p = 0.002$). In contrast, the score for patchy abnormalities was similar among both readers (9 ± 8.3 vs. 10.5 ± 7.5; $p = 0.248$, a table with full details on scoring of all patients by the two readers is available as electronic Supplementary material 4).

Abnormalities on IDIs consistent with pulmonary emphysema were seen in 13 (Reader 1) respectively in 14 patients (Reader 2).

4. Discussion

While the value of CTPA for the diagnosis of CTEPH is well established [10], the added value of multi-energy CT acquisitions for the diagnostic workup of patients with suspected pulmonary hypertension has only been evaluated in a small number of studies, none of them using the dual-layer technology of the SDCT.

Our results demonstrate that SDCT may serve as a valuable tool in the diagnosis of CTEPH with excellent sensitivity and specificity. These results are in line with Dournes et al. and Masy et al. who both reported similar high sensitivities and specificities for the diagnosis for CTEPH by using dual-energy dual-source CT technology [11,14].

Compared to an analysis of CTPA images alone, iodine density and monoenergetic images improved specificity for the diagnosis of CTEPH for both readers and greatly improved sensitivity for the detection of CTEPH for the less experienced reader. Furthermore, the access to SDCT data significantly increased diagnostic confidence for both readers. This shows that the additional image information provided by SDCT may prove especially helpful for radiologists, who do not read CTPA studies of patients with PH on a regular basis, by increasing diagnostic accuracy and confidence.

The increase in specificity for a diagnosis of CTEPH, in particular, underlines that an analysis of perfusion patterns on IDIs may help in differentiating the various etiologies of PH. When analyzing perfusion patterns, it is important to keep in mind that changes in iodine distribution can be caused by a variety of non-vascular causes [23] and thus findings on IDIs need to be correlated with vascular findings and changes of the lung parenchyma. In contrast to Masy et al. [14] we did not exclude any patients because of infiltrative or destructive lung changes and our patient cohort included a significant number of patients with signs of pulmonary emphysema and corresponding abnormalities on IDIs, but these were identified with confidence by both readers. Confirming reports by Kim et al. [15] and Giordano et al. [16] on perfusion patterns in dual-energy CTs, we found embolic and regional perfusion defects to be nearly exclusively prevalent in CTEPH patients. In contrast, patchy perfusion abnormalities predominated in patients with a pre- or postcapillary etiology but were also present in patients with CTEPH to a lesser extent.

In addition to enabling a better differentiation of disease etiologies, IDIs carry the potential for a better quantification of perfusion abnormalities as a non-invasive derivative for disease severity. Meinel et al. demonstrated an automated pulmonary blood volume (PBV) scoring for dual-energy CT based IDIs that correlated well with the mPAP in CTEPH patients [24].

For the current lack of clinically available software tools allowing a volumetric quantification of iodine content on our SDCT platform we resorted to a previously suggested [17] semi-quantitative scoring of perfusion defects in our study. Accordingly, readers were asked to decide by visual rating whether more or <50% of a pulmonary segment was affected by hypoperfusion. By this approach, we were able to demonstrate a significant, though weak, correlation between the extent of perfusion abnormalities and the mPAP in patients with PH other than CTEPH. For CTEPH patients however, no significant correlation was found, consistent with a report by Hoey et al. [25]. In contrast, Takagi et al. were able to show a significant correlation between the extent of perfusion abnormalities and severity of disease (most importantly based on the mPAP) [17]. However, there are important differences between Takagi et al. and our study. Firstly, Takagi et al. also included a significant number of patients who had mPAP values of <25 mm Hg under therapy. Secondly, they used a significantly shorter scan delay of 1 s compared to the 4.9 s employed by us, thus limiting the amount of iodine in the lung parenchyma provided by systemic arterial collaterals.

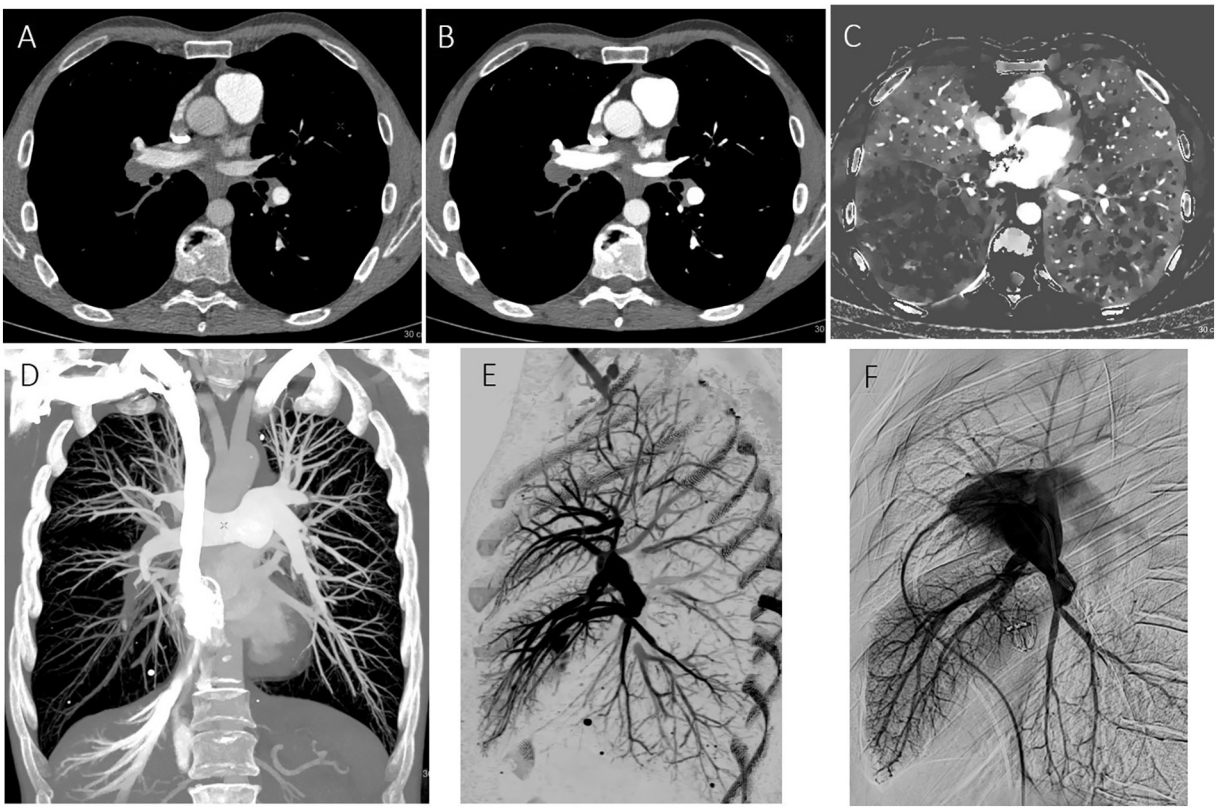

Fig. 3. Exemplary images of a CTEPH patient. Example of patient with CTEPH with a thrombotic occlusion of the interlobar artery (A, conventional CTPA). Image B highlights the enhanced attenuation of the pulmonary vasculature on monoenergetic images (50 keV) while C displays the regional perfusion defect of the right lower lobe and patchy perfusion abnormalities especially in the left lower lobe on iodine density images. D shows a maximum intensity projection reconstruction of monoenergetic images again showing the great vessel contrast. Image E shows the right pulmonary artery in a lateral view in an iodine density angiogram (inverted maximum intensity projection of iodine density images) in comparison to a digital subtraction angiogram with selective catherization of the right pulmonary artery.

This might have led to an underestimation of the severity of perfusion defects in our study.

One limitation of our study is the relatively small sample size which is explained by the only recent availability of SDCT technology and the relative scarcity of patients with PH. We did not include a healthy control cohort but wanted to show the strength of SDCT in a real-world scenario where the differentiation between patients with CTEPH from patients with other forms of PH or patients with other pulmonary or cardiovascular diseases is more important than the differences between CTEPH patients and a healthy cohort. For correlation analysis between SDCT and RHC we arbitrarily restricted the acceptable interval between both examinations to a maximum of 5 days and excluded any patient with a longer interval from correlation analysis. However, even with a mean interval of 1.2 days between the examinations there still might be relevant changes in pulmonary pressure and lung perfusion because of the complex pulmonary hemodynamics. Although a semi-quantitative scoring of IDIs shows some promise for PH patients in quantifying the extent of the disease based on CT data, it is still time consuming and remains of limited accuracy. A visual analysis can only give a rough estimate. Moreover, inter-reader reproducibility is a major concern of visual rating, as highlighted by the difference in the scoring of perfusion deficits by our two readers. Even with significantly different scores for embolic and regional perfusion defects for both readers though, these perfusion defects were significantly more common in patients with CTEPH even when looking at each reader's scoring results independently. This highlights the robustness of these scores even when the assessment of severity of perfusion abnormalities remains subjective. We believe that volumetric iodine quantification and comprehensive analysis of IDIs employing Radiomics might further facilitate the value of SDCT for a better and more objective severity assessment in patients with PH.

A major limitation of the current SDCT platform is that spectral image information can only be generated if patients are scanned at 120 kV. This limits the possibility to reduce radiation dose by using lower kV settings especially for patients with lower BMI. In addition, using lower kV settings would enhance iodine contrast and thus is especially useful in CT angiography. Nevertheless, SDCT allows for a similar effect by using virtual monoenergetic images which allow low keV images with stable images noise compared to standard images [26]. Hopefully, further development of SDCT might overcome this limitation.

In conclusion, SDCT offers a highly accurate way to diagnose CTEPH and should be considered as a primary tool in the diagnostic work-up of patients with suspected PH as it allows for comprehensive analysis of the pulmonary vasculature, the lung parenchyma and the pulmonary perfusion in a single examination (an exemplary case presented in Fig. 3 highlights the value of SDCT). The right timing and optimal contrast injection protocol detection of PH induced perfusion abnormalities remain elusive and more sophisticated automated analysis of IDIs might improve the value of SDCT for this patient group. The semi-quantitative analysis in our study was not able to differentiate non-CTEPH groups any further. The extent of perfusion abnormalities correlated only weakly with the mPAP in our patients. In the future, more sophisticated quantitative analyses including Radiomics might help a better differentiation of etiologies and disease severities. Thus, SDCT holds promise to become a one-stop study for patients with PH with a potential of making V/Q-scintigraphy obsolete.

Supplementary data to this article can be found online at https://doi.org/10.1016/j.ijcard.2019.03.018.

Conflict of interest

Jan Robert Kröger received a research grant from Philips Healthcare, Netherlands in 2017. Except for this funding Philips Healthcare was not involved in any aspects of the presented study.

The other authors report no relationships that could be construed as a conflict of interest.

References

[1] N. Galiè, M. Humbert, J.-L. Vachiery, et al., 2015 ESC/ERS guidelines for the diagnosis and treatment of pulmonary hypertension, Eur. Heart J. 37 (2015) 67–119.
[2] M.A. Gatzoulis, I. Adatia, D. Celermajer, et al., Updated clinical classification of pulmonary hypertension, J. Am. Coll. Cardiol. 62 (2013) D34–D41.
[3] S. Rosenkranz, H.A. Ghofrani, E. Grünig, et al., Cologne consensus conference on pulmonary hypertension – update 2018, Int. J. Cardiol. 272 (2018) 1–3.
[4] E. Mayer, D. Jenkins, J. Lindner, et al., Surgical management and outcome of patients with chronic thromboembolic pulmonary hypertension: results from an international prospective registry, J. Thorac. Cardiovasc. Surg. 141 (2011) 702–710.
[5] A.K. Andreassen, A. Ragnarsson, E. Gude, et al., Balloon pulmonary angioplasty in patients with inoperable chronic thromboembolic pulmonary hypertension, Heart 99 (2013) 1415–1420.
[6] H. Wilkens, S. Konstantinides, I.M. Lang, et al., Chronic thromboembolic pulmonary hypertension (CTEPH): updated recommendations from the Cologne consensus conference 2018, Int. J. Cardiol. 272 (2018) 69–78.
[7] N. Tunariu, S.J.R. Gibbs, Z. Win, et al., Ventilation-perfusion scintigraphy is more sensitive than multidetector CTPA in detecting chronic thromboembolic pulmonary disease as a treatable cause of pulmonary hypertension, J. Nucl. Med. 48 (2007) 680–684.
[8] F.R. Gutierrez, F.G.D. Telli, S.Y. Aravena, Approach to pulmonary hypertension: from CT to clinical diagnosis, RadioGraphics 1 (2018) 17.
[9] J. He, W. Fang, B. Lv, et al., Diagnosis of chronic thromboembolic pulmonary hypertension, Nucl. Med. Commun. 33 (2012) 459–463.
[10] C. Dong, M. Zhou, D. Liu, et al., Diagnostic accuracy of computed tomography for chronic thromboembolic pulmonary hypertension: a systematic review and meta-analysis, PLoS One 10 (2015), e0126985.
[11] G. Dournes, D. Verdier, M. Montaudon, et al., Dual-energy CT perfusion and angiography in chronic thromboembolic pulmonary hypertension: diagnostic accuracy and concordance with radionuclide scintigraphy, Eur. Radiol. 24 (2014) 42–51.
[12] S.F. Thieme, C.R. Becker, M. Hacker, et al., Dual energy CT for the assessment of lung perfusion—correlation to scintigraphy, Eur. J. Radiol. 68 (2008) 369–374.
[13] T. Nakazawa, Y. Watanabe, Y. Hori, et al., Lung perfused blood volume images with dual-energy computed tomography for chronic thromboembolic pulmonary hypertension: correlation to scintigraphy with single-photon emission computed tomography, J. Comput. Assist. Tomogr. 35 (2011) 590–595.
[14] M. Masy, J. Giordano, G. Petyt, et al., Dual-energy CT (DECT) lung perfusion in pulmonary hypertension: concordance rate with V/Q scintigraphy in diagnosing chronic thromboembolic pulmonary hypertension (CTEPH), Eur. Radiol. (2018) 1–11.
[15] E.Y. Kim, J.B. Seo, S.Y. Oh, et al., Assessment of perfusion pattern and extent of perfusion defect on dual-energy CT angiography: correlations between the causes of pulmonary hypertension and vascular parameters, Korean J. Radiol. 15 (2014) 286–294.
[16] J. Giordano, S. Khung, A. Duhamel, et al., Lung perfusion characteristics in pulmonary arterial hypertension (PAH) and peripheral forms of chronic thromboembolic pulmonary hypertension (pCTEPH): dual-energy CT experience in 31 patients, Eur. Radiol. 27 (2017) 1631–1639.
[17] H. Takagi, H. Ota, K. Sugimura, et al., Dual-energy CT to estimate clinical severity of chronic thromboembolic pulmonary hypertension: comparison with invasive right heart catheterization, Eur. J. Radiol. 85 (2016) 1574–1580.
[18] R.E. Alvarez, A. MacOvski, Energy-selective reconstructions in X-ray computerised tomography, Phys. Med. Biol. 21 (1976) 733–744.
[19] F.A. Dilmanian, X.Y. Wu, E.C. Parsons, et al., Single- and dual-energy CT with monochromatic synchrotron x-rays, Phys. Med. Biol. 42 (1997) 371–387.
[20] J. Doerner, M. Hauger, T. Hickethier, et al., Image quality evaluation of dual-layer spectral detector CT of the chest and comparison with conventional CT imaging, Eur. J. Radiol. 93 (2017) 52–58.
[21] J.R. Kröger, T. Hickethier, G. Pahn, et al., Influence of spectral detector CT based monoenergetic images on the computer-aided detection of pulmonary artery embolism, Eur. J. Radiol. 95 (2017) 242–248.
[22] A. Ruggiero, N.J. Screaton, Imaging of acute and chronic thromboembolic disease: state of the art, Clin. Radiol. 72 (2017) 375–388.
[23] B.H. Kim, J.B. Seo, E.J. Chae, et al., Analysis of perfusion defects by causes other than acute pulmonary thromboembolism on contrast-enhanced dual-energy CT in consecutive 537 patients, Eur. J. Radiol. 81 (2012) e647–e652.
[24] F.G. Meinel, A. Graef, K.M. Thierfelder, et al., Automated quantification of pulmonary perfused blood volume by dual-energy CTPA in chronic thromboembolic pulmonary hypertension, RöFo 186 (2014) 151–156.
[25] E.T.D. Hoey, S. Mirsadraee, J. Pepke-Zaba, et al., Dual-energy CT angiography for assessment of regional pulmonary perfusion in patients with chronic thromboembolic pulmonary hypertension: initial experience, Am. J. Roentgenol. 196 (3) (2011) 524–532.
[26] D. Sakabe, Y. Funama, K. Taguchi, et al., Image quality characteristics for virtual monoenergetic images using dual-layer spectral detector CT: comparison with conventional tube-voltage images, Phys. Med. 49 (2018) 5–10.